



Kinematics of wheeled mobile robots on uneven terrain

Nilanjan Chakraborty, Ashitava Ghosal *

Department of Mechanical Engineering, Indian Institute of Science, Bangalore 560012, India

Accepted 25 May 2004

Available online 1 October 2004

Abstract

This paper deals with the kinematic analysis of a wheeled mobile robot (WMR) moving on uneven terrain. It is known in literature that a wheeled mobile robot, with a fixed length axle and wheels modeled as thin disk, will undergo slip when it negotiates an uneven terrain. To overcome slip, variable length axle (VLA) has been proposed in literature. In this paper, we model the wheels as a torus and propose the use of a passive joint allowing a lateral degree of freedom. Furthermore, we model the mobile robot, instantaneously, as a hybrid-parallel mechanism with the wheel–ground contact described by differential equations which take into account the geometry of the wheel, the ground and the non-holonomic constraints of no slip. We present an algorithm to solve the direct and inverse kinematics problem of the hybrid-parallel mechanism involving numerical solution of a system of differential-algebraic equations. Simulation results show that the three-wheeled WMR with torus shaped wheels and passive joints can negotiate uneven terrain without slipping. Our proposed approach presents an alternative to variable length axle approach. © 2004 Elsevier Ltd. All rights reserved.

1. Introduction

In this paper we address the problem of motion of wheeled mobile robots on uneven terrain without kinematic slip. The motion of wheeled mobile robots (WMR) on flat terrain has been well studied in [1,2]. Waldron [3] has argued that two wheels independently joined to a common axle

* Corresponding author. Tel.: +91 80 394 2956; fax: +91 80 293 2956.
E-mail address: asitava@mecheng.iisc.ernet.in (A. Ghosal).

cannot roll on uneven terrain without slip. The use of Ackerman steering and differential wheel actuation which works for conventional vehicles on flat terrain does not work because there is no instantaneous center compatible with both wheels. The lateral slip in WMR's is undesirable because it leads to *localization* errors thus increasing the burden on sensor based navigation algorithms. In addition, for planetary explorations, power is at a premium and such slipping leads to large wastage of power.

The problem of two wheels joined independently to an axle, moving on uneven terrain without slip, has been studied by Sreenivasan et al. [4–8]. They have modeled the vehicles as hybrid series–parallel chains and using instantaneous rate kinematics showed that for prevention of slip, (a) the line joining the wheel terrain contact points must be coplanar with the axle axis, or (b) the wheels must be driven at identical speeds relative to the axle. For prevention of slip they have suggested the use of a variable length axle (VLA), wherein an unactuated prismatic joint is used in the axle to vary axle length.

There are a few limitations of using a VLA—(a) at high inclinations there is slipping due to gravity loading, and (b) the dynamic slip due to inertial loading becomes large at higher speeds. To overcome the limitations in VLA, the use of an actuated VLA has been proposed. An actuated VLA, however, requires accurate measurement of slip to obtain the desired actuator output.

It may be noted that all the above mentioned work model the wheel as a thin disk. On a flat ground this is reasonable since the contact point always lies in a vertical plane passing through the center of the wheel. However on uneven terrain this is not the case in general and the contact point will vary along the lateral surface of a general wheel due to terrain geometry variations.

In this paper we have proposed an alternative to VLA for slip-free motion capability in wheeled mobile robots. Our alternative design is based on the following concepts:

- Each wheel is assumed to be a torus. The wheels and the ground are considered as rigid bodies and single point contact is assumed between the wheel and the ground. The equations describing the geometry of the wheel and the ground are assumed to be sufficiently smooth and continuous such that derivatives up to second-order exists and geometric properties such as curvature and torsion can be computed.
- The equations of contact between two arbitrary surfaces in single point contact, derived by Montana [9], are used to model the contact of a torus shaped wheel on an uneven terrain. The ordinary differential equations (ODE's) describing the no-slip motion of the torus shaped wheel on the uneven ground are derived from the equations of contact.
- The lateral rotational motion of the wheel is accommodated by a *passive* rotary joint. This allows the distance between the wheel–ground contact points to change without changing the axle length. Since this joint is passive, sensing or control is not required.
- *Instantaneously*, the wheeled mobile robot is modeled as hybrid-parallel mechanism with a three-degree-of-freedom joint at the wheel–ground contact. Unlike a typical kinematic joint, the *no-slip* non-holonomic constraint leads to non-linear ordinary differential equations.
- The direct and inverse kinematics problem for the mobile robot is formulated as a set of ODE's and numerically solved by integrating the ODE's and the holonomic constraints arising out of the hybrid-parallel mechanism.

We demonstrate our approach with a 3-wheeled vehicle and show by simulation that slip free motion can be achieved without a passive or actuated VLA. In our approach, no-slip motion is achieved by using torus shaped wheels and passive rotary joints without any additional sensors or control. This is the main contribution of this paper.

The paper is organized as follows: in the next section, we obtain the contact equations for a single torus shaped wheel moving on an uneven terrain. In Section 3, we present our approach of modeling of the three-wheeled WMR as a hybrid-parallel manipulator instantaneously and derive the direct and inverse kinematic equations. In Section 4, we present simulation results, illustrating the capability of the WMR to negotiate uneven terrain without slip. In the last section we present the conclusions.

2. Kinematic modeling of a single wheel

For a smooth surface given in the parametric form, $(x, y, z)^T = \mathbf{X}(u, v)$, the metric, curvature and torsion for the surface is defined by

$$[M] = \begin{bmatrix} |\mathbf{X}_u| & 0 \\ 0 & |\mathbf{X}_v| \end{bmatrix} \quad [K] = \begin{bmatrix} -\mathbf{X}_{uu} \cdot \mathbf{n}/|\mathbf{X}_u| & -\mathbf{X}_{uv} \cdot \mathbf{n}/|\mathbf{X}_v| \\ -\mathbf{X}_{uv} \cdot \mathbf{n}/|\mathbf{X}_u| & -\mathbf{X}_{vv} \cdot \mathbf{n}/|\mathbf{X}_v| \end{bmatrix}$$

$$[T] = [\mathbf{X}_v \cdot \mathbf{X}_{uu}/|\mathbf{X}_u| \quad \mathbf{X}_v \cdot \mathbf{X}_{uv}/|\mathbf{X}_v|] \quad \text{where } \mathbf{n} = \frac{\mathbf{X}_u \times \mathbf{X}_v}{|\mathbf{X}_u \times \mathbf{X}_v|}$$

where $\mathbf{X}_{(\cdot)}$ and $\mathbf{X}_{(\cdot)(\cdot)}$ denote first and second partial derivatives. We assume that we have a digital elevation model (DEM) of the ground i.e. n available measured data points given in the form $(x, y, z)_i, i = 1, 2, \dots, n$. For our analysis, we require a surface representation which is at least \mathcal{C}^2 continuous. Without loss of generality we represent the uneven surface using a bi-cubic patch given by

$$\mathbf{X}(u, v) = \sum_{i=0}^3 \sum_{j=0}^3 a_{ij} u^i v^j \quad (u, v) \in [0, 1]$$

The coefficients a_{ij} are determined if 16 data points are known (for details, see [10]). For our simulation purposes we have assumed synthetic ground data and have used in-built functions in Matlab [11] (Spline Tool Box) to generate a bi-cubic patch from the n given data points.

Fig. 1 shows a torus wheel on an uneven ground. The frames $\{0\}$ and $\{w\}$ are fixed to the ground and wheel respectively. The frames $\{1\}$ and $\{2\}$ are the Gaussian frames at the point of contact on the ground and wheel, respectively, fixed with respect to the body frames. The four parameters $(u_1, v_1), (u_g, v_g)$ (point of contact on surfaces 1 and 2 in $\{w\}$ and $\{0\}$ respectively) and the angle ψ between the X -axis of $\{1\}$ and $\{2\}$ are the five degrees of freedom between the two contacting surfaces. The angle ψ is chosen such that a rotation by angle $-\psi$ aligns the two X -axes.

The equation of the torus shaped wheel in $\{w\}$ in terms of parameters (u_1, v_1) can be written as

$$(x, y, z) = (r_1 \cos u_1, \cos v_1 (r_2 + r_1 \sin u_1), \sin v_1 (r_2 + r_1 \sin u_1)) \tag{1}$$

and the equation of the uneven ground is given by $(x, y, z) = (u_g, v_g, f(u_g, v_g))$.

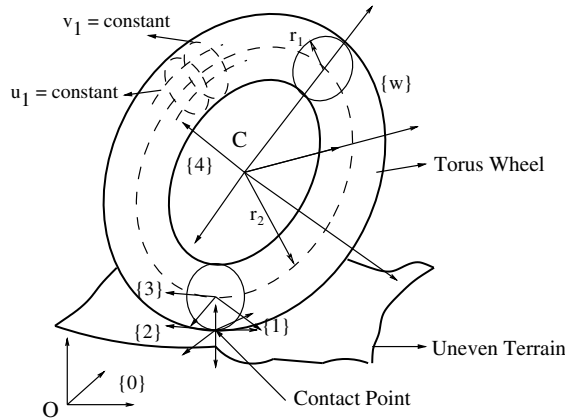


Fig. 1. Torus wheel on uneven ground.

The 4×4 homogeneous transformation matrix, ${}^0_w[T]$, describing the position and orientation of the co-ordinate system $\{w\}$ with respect to the fixed co-ordinate system $\{0\}$ is given by the product ${}^0_1[T]{}^1_2[T]{}^2_3[T]{}^3_4[T]{}^4_w[T]$ (see Fig. 1). The matrix ${}^0_1[T]$ describes the uneven ground at wheel-ground contact point, and denoting the equation of the uneven ground by $(u_g, v_g, f(u_g, v_g))^T$, the matrix ${}^0_1[T]$ is given by

$${}^0_1[\mathbf{T}] = \begin{pmatrix} l_1 & m_1 & n_1 & u_g \\ l_2 & m_2 & n_2 & v_g \\ l_3 & m_3 & n_3 & f(u_g, v_g) \\ 0 & 0 & 0 & 1 \end{pmatrix}$$

where $l_i, m_i, n_i, i = 1, 2, 3$ are the components of the orthogonal vectors $\{\frac{\mathbf{f}_{g_u}}{|\mathbf{f}_{g_u}|}, \frac{\mathbf{n} \times \mathbf{f}_{g_u}}{|\mathbf{n} \times \mathbf{f}_{g_u}|}, \mathbf{n}\}$ respectively. The transformation ${}^1_2[T]$ describes the ψ rotation of the wheel. The transformation matrices ${}^2_3[T]$ and ${}^3_4[T]$ describe the tilt and rotation of the torus shaped wheel respectively. The final ${}^4_w[T]$ constant matrix ensures that Z-axis (of the torus-wheel) is pointed vertically up wards. The transformation matrices are given as

$${}^1_2[\mathbf{T}] = \begin{pmatrix} \cos \psi & -\sin \psi & 0 & 0 \\ -\sin \psi & -\cos \psi & 0 & 0 \\ 0 & 0 & -1 & 0 \\ 0 & 0 & 0 & 1 \end{pmatrix}, \quad {}^2_3[\mathbf{T}] = \begin{pmatrix} \sin u & 0 & \cos u & 0 \\ 0 & 1 & 0 & 0 \\ -\cos u & 0 & \sin u & -r_1 \\ 0 & 0 & 0 & 1 \end{pmatrix},$$

$${}^3_4[\mathbf{T}] = \begin{pmatrix} 1 & 0 & 0 & 0 \\ 0 & -\sin v & \cos v & 0 \\ 0 & -\cos v & -\sin v & -r_2 \\ 0 & 0 & 0 & 1 \end{pmatrix}, \quad {}^4_w[\mathbf{T}] = \begin{pmatrix} -1 & 0 & 0 & 0 \\ 0 & 1 & 0 & 0 \\ 0 & 0 & -1 & 0 \\ 0 & 0 & 0 & 1 \end{pmatrix}$$

The contact between two smooth surfaces have been obtained by Montana [9]. For our case of the torus shaped wheel and the smooth uneven ground, we have

$$\begin{aligned}
 (\dot{u}_1, \dot{v}_1)^T &= [M_1]^{-1}([K_1] + [K^*])^{-1}[(-\omega_y, \omega_x)^T - [K^*](v_x, v_y)^T] \\
 (\dot{u}_g, \dot{v}_g)^T &= [M_g]^{-1}[R_\psi]([K_1] + [K^*])^{-1}[(-\omega_y, \omega_x)^T + [K_1](v_x, v_y)^T] \\
 \dot{\psi} &= \omega_z + [T_1][M_1](\dot{u}_1, \dot{v}_1)^T + [T_g][M_g](\dot{u}_g, \dot{v}_g)^T \\
 0 &= v_z
 \end{aligned} \tag{2}$$

where

$$[K^*] = [R_\psi][K_g][R_\psi]^T, \quad [R_\psi] = \begin{pmatrix} \cos \psi & -\sin \psi \\ -\sin \psi & -\cos \psi \end{pmatrix},$$

ω_x, ω_y and ω_z are the angular velocity and v_x, v_y and v_z are the linear velocity components of {2} relative to {1}, expressed in {2}. For rolling without slip v_x, v_y should be zero.

In Eq. (2), $[M_1], [K_1], [T_1]$ are the metric, curvature and the torsion of the wheel respectively. They can be computed from the equation of the torus, Eq. (1), and are given as

$$\begin{aligned}
 [M_1] &= \begin{bmatrix} r_1 & 0 \\ 0 & r_2 + r_1 \sin u_1 \end{bmatrix} \\
 [K_1] &= \begin{bmatrix} \frac{1}{r_1} & 0 \\ 0 & \frac{\sin u_1}{r_2 + r_1 \sin u_1} \end{bmatrix} \\
 [T_1] &= \begin{bmatrix} 0 & \frac{\cos u_1}{r_2 + r_1 \sin u_1} \end{bmatrix}
 \end{aligned} \tag{3}$$

In Eq. (2), $[M_g], [K_g], [T_g]$ are the metric, curvature and the torsion of the uneven ground. Depending on the cubic surface chosen to represent the uneven ground, the expression for these quantities were computed in closed form using Mathematica [12].

3. Kinematic modeling of 3-wheeled WMR

We now consider the modeling of a 3-wheeled vehicle moving on uneven terrain without slip. For this, we assume that the rear wheels have a degree-of-freedom at the wheel axle joint allowing lateral tilt. The axis of lateral tilt is perpendicular to the axle joining the two rear wheels along the plane of the platform. The front wheel can be steered and it has no lateral tilt capability. In this configuration, we can model the vehicle instantaneously as an equivalent hybrid-parallel mechanism as shown in Fig. 2. As mentioned in Eq. (2), at the wheel-ground contact point, we have one holonomic constraint, $v_z = 0$, which ensures wheel-ground contact is always maintained. Moreover, at each instant, we have 2 non-holonomic constraints which prevents instantaneous sliding, and these are $v_x = 0$ and $v_y = 0$. Intuitively, this suggests us to model the wheel ground contact

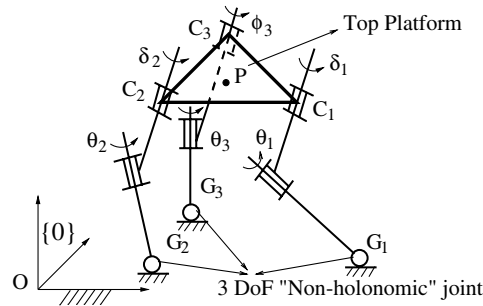


Fig. 2. Equivalent instantaneous mechanism for 3-wheeled WMR.

point, *instantaneously*, as a three-degree-of-freedom (DOF) joint. It may be noted that this joint is different from a three-DOF spherical joint since the two non-holonomic constraints restrict the motion at any instant *only* in terms of achievable velocities.¹ In addition, the wheel–axle joints allowing rotation of the wheel, lateral tilt and steering respectively are modeled as 1 DOF rotary (*R*) joints. Using Gruebler’s formula

$$\text{DOF} = 6(n - j - 1) + \sum f_i$$

we obtain the degrees of freedom of the top platform as 3, with the total number of links n as 8, number of joints j as 9, and the total number of degrees of freedom (3 for each wheel–ground contact and 1 for each of the 6 rotary joints), $\sum f_i = 15$. Therefore, three of the joint variables should be actuated and we choose rotation at the two rear wheels, θ_1 and θ_2 , and the steering at the front wheel, ϕ_3 , as the actuated variables. The two lateral tilts at the rear wheels, δ_1 and δ_2 , and the rotation of the front wheel θ_3 are passive variables which need to be computed from kinematics.

As the vehicle is subjected to non-holonomic (and thereby non-integrable) no-slip constraints, the kinematics problem can at best be formulated in terms of the first derivatives of the joint variables and the joint variables are obtained by integration. The direct and inverse kinematics problem for the 3-DOF vehicle can be stated as follows:

- *Direct kinematics problem:* Given the actuated variables as a function of time, t , $\dot{\theta}_1(t)$, $\dot{\theta}_2(t)$, $\dot{\phi}_3(t)$, and the geometrical properties of the uneven ground and wheel, obtain the resulting orientation of the top platform in terms of a rotation matrix ${}^0_p[R]$ (or a suitable parametrization of it) and the position of the center of the platform (or any other point of interest).
- *Inverse kinematics problem:* Given any three of the components of the linear and angular velocity (as a function of time) of the top platform $V_x, V_y, V_z, \Omega_x, \Omega_y, \Omega_z$ (V_x, V_y, V_z are the components of the linear velocity vector of the center of the platform or any other point of interest and $\Omega_x, \Omega_y, \Omega_z$ are the components of the angular velocity vector of the platform) and the

¹ As known in literature, non-holonomic constraints restrict only the space of achievable velocities and *not* the positions. A wheel or a thin disk undergoing rolling without slip, with $v_x = v_y = 0$, can reach any position in a plane and the only constraint is that of not leaving the plane and loosing contact.

geometric properties of the ground and wheel, obtain the two drive inputs to the rear wheels, $\theta_1(t)$, $\theta_2(t)$, and the steering input to the front wheel, $\phi_3(t)$, which yield the three given velocity components of the top platform.²

To solve the above two problems we proceed as follows:

1. *Generate surface*

As described in Section 2, we use 2-D cubic splines to reconstruct the surface from given elevation data. From the interpolated surface we obtain expressions for the metric, curvature and torsion form for the ground using Mathematica [12].

2. *Form contact equations*

For each wheel we write the 5 differential equations (see Eq. (2)) in the 15 contact variables u_i , v_i , u_{g_i} , v_{g_i} , and ψ_i , where $i = 1, 2, 3$. Since the wheels undergo no-slip motion, we set $v_x = v_y = 0$ for each of the wheels. It may be noted that ω_x , ω_y and ω_z in the contact equations for each wheel are the three components of angular velocities of frame {2} with respect to frame {1} and are unknown. These are related to the angular velocity of the platform Ω_x , Ω_y , Ω_z and the input and passive joint rates. In the fixed coordinate system, {0}, we can write

$${}^0(\omega_x, \omega_y, \omega_z)^T = {}^0(\Omega_x, \Omega_y, \Omega_z)^T + {}^0\omega_{\text{input}} \tag{4}$$

where ${}^0\omega_{\text{input}} = {}^0[\dot{R}]_{\text{in}} {}^0[R]_{\text{in}}^T$ with ${}^0[R]_{\text{in}}$ given by ${}^0_p[R][R(\mathbf{e}_2, \delta_i)][\mathbf{R}(\mathbf{e}_1, \theta_i)]$ for $i = 1, 2$ and by ${}^0_p[R][R(\mathbf{e}_3, \phi_i)][\mathbf{R}(\mathbf{e}_1, \theta_i)]$ for $i = 3$, and $\mathbf{e}_1 = (\mathbf{1}, \mathbf{0}, \mathbf{0})^T$, $\mathbf{e}_2 = (\mathbf{0}, \mathbf{1}, \mathbf{0})^T$, $\mathbf{e}_3 = (\mathbf{0}, \mathbf{0}, \mathbf{1})^T$. The above Eq. (4) couples all 5 sets of ODE's and we get a set of 15 coupled ODE's in 21 variables. These are the 15 contact variables u_i , v_i , u_{g_i} , v_{g_i} , ψ_i ($i = 1, 2, 3$), the 3 wheel rotations θ_1 , θ_2 , θ_3 , the 2 lateral tilts δ_1 , δ_2 , and the front wheel steering ϕ_3 .

3. *Obtain velocity of platform*

The angular velocity and the linear velocity of the center of the platform are expressed in terms of the 15 wheel variables u_i , v_i , u_{g_i} , v_{g_i} , ψ_i ($i = 1, 2, 3$). If γ , β , α be a 3–2–1 Euler angle parametrization representing the orientation of the platform we have

$$\begin{aligned} {}^0\Omega_x &= \dot{\alpha} \cos(\beta) \cos(\gamma) - \dot{\beta} \sin(\gamma) = f_1(u_i, v_i, u_{g_i}, v_{g_i}, \psi_i) \\ {}^0\Omega_y &= \dot{\alpha} \cos(\beta) \sin(\gamma) + \dot{\beta} \cos(\gamma) = f_2(u_i, v_i, u_{g_i}, v_{g_i}, \psi_i) \\ {}^0\Omega_z &= \dot{\gamma} - \dot{\alpha} \sin(\beta) = f_3(u_i, v_i, u_{g_i}, v_{g_i}, \psi_i) \end{aligned} \tag{5}$$

If x_c , y_c , z_c denotes the coordinates of the center of the platform in {0}. The linear velocity of the center of the platform is given by

$${}^0(V_x, V_y, V_z)^T = (\dot{x}_c, \dot{y}_c, \dot{z}_c)^T = V_{w_i} + {}^0(\Omega_x, \Omega_y, \Omega_z)^T \times {}^0R_{c_i} \tag{6}$$

where i stands for any one of the 3 wheels 1, 2 or 3 and ${}^0R_{c_i}$ is the point of attachment of the wheel to the platform from the center of the platform expressed in frame {0}.

² Instead of the angular velocities Ω_x , Ω_y , Ω_z , we may use the Euler angle rates $\dot{\alpha}$, $\dot{\beta}$, $\dot{\gamma}$, where γ , β , α is a 3–2–1 Euler angle parametrization of orientation.

4. Form holonomic constraint equations

In addition to the contact equations, for the 3 wheels to form a vehicle the distance between the 3 points C_1, C_2, C_3 (refer to Fig. 2) must remain constant. These holonomic constraint equations can be written as

$$(\overrightarrow{OC_1} - \overrightarrow{OC_2})^2 = l_{12}^2; \quad (\overrightarrow{OC_1} - \overrightarrow{OC_3})^2 = l_{13}^2; \quad (\overrightarrow{OC_3} - \overrightarrow{OC_2})^2 = l_{32}^2; \quad (7)$$

where $\overrightarrow{OC_1}, \overrightarrow{OC_2}, \overrightarrow{OC_3}$ are the position vectors of the center of the three wheels, C_1, C_2, C_3 , respectively from the origin \mathbf{O} of the fixed frame and l_{ij} is the distance between center of wheels i and j respectively.

3.1. Solution of the direct kinematics problem

From steps 1, 2, 4 we have 15 first order ODE's and 3 algebraic constraint equations for the 18 unknown variables ($\theta_1, \theta_2, \phi_3$ are given). This system of differential algebraic equations (DAE's) can be converted to 18 ODE's in 18 variables by differentiating the constraint equations. It is to be noted that the 18 ODE's have been derived symbolically using the symbolic manipulation package Mathematica [12]. Using an ODE solver, we solve the set of 18 ODE's numerically, with the initial conditions obtained as outlined below. Once we have obtained $u_i, v_i, u_{g_i}, v_{g_i}, \psi_i, i = 1, 2, 3$ and $\delta_1, \delta_2, \theta_3$ we can obtain the rotation matrix of the platform ${}^0_p[R]$. The position vector of the center of the platform \overrightarrow{OP} with respect to the fixed frame, $\{0\}$, denoted by (x_c, y_c, z_c) is given by (see Fig. 2)

$$(x_c, y_c, z_c)^T = \overrightarrow{OC_i} + {}^0_p[R] \overrightarrow{C_iP} \quad \text{for any } i = 1, 2 \text{ or } 3. \quad (8)$$

3.2. Solution of the inverse kinematics problem

From steps 1, 2, 3, 4 we have 21 first order ODE's and 3 algebraic constraints for 24 unknowns (in this case we assume $\dot{x}_c, \dot{y}_c, \dot{\gamma}$ are given). This set of DAE's is also converted to ODE's and integrated using initial conditions determined as discussed below. Numerical solution gives the 15 contact variables $u_i, v_i, u_{g_i}, v_{g_i}, \psi_i, i = 1, 2, 3$, the 3 actuated variables $\theta_1, \theta_2, \phi_3$ and the 3 passive variables $\delta_1, \delta_2, \theta_3$. The other 3 platform variables z_c, α, β are also obtained.

3.3. Initial conditions

To solve the set of ODE's in direct or inverse kinematics problem, we have to choose the initial conditions such that it satisfies the holonomic constraint equations. For the direct kinematics among the 18 variables we can choose $\delta_1 = 0, \delta_2 = 0, \theta_3 = 0$, initially. Moreover we can also choose v_1, v_2, v_3 to be $3\pi/2$ and the position of point of contact of any one wheel in $\{0\}$ (in our simulations, we have chosen the point of contact of wheel 2, given by u_{g_2}, v_{g_2}). The other two wheels must also be in contact with the uneven ground. Hence, for each wheel, we have

$$\overrightarrow{OC_i} + {}^0_w[\mathbf{R}] \cdot \overrightarrow{C_iG_i} = \overrightarrow{OG_i}; \quad i = 1, 2, 3 \quad (9)$$

Converting them to unit vectors we have two independent equations for each wheel. In addition, for each of the three wheels, we have,

$$\cos(\psi_i) = \hat{e}_{1_i} \cdot \hat{e}'_{1_i} \quad i = 1, 2, 3 \tag{10}$$

where $\{\hat{e}_1, \hat{e}_2, \hat{e}_3\}$ and $\{\hat{e}'_1, \hat{e}'_2, \hat{e}'_3\}$ are the coordinate axes of reference frames $\{2\}$ and $\{1\}$ respectively in $\{0\}$ (refer to Fig. 1). Finally there are 3 holonomic constraint equations given by Eq. (7). This gives us a set of 10 nonlinear equations in 10 variables and this set is solved numerically to yield consistent initial conditions for the direct kinematics problem.

For inverse kinematics problem involving 24 ODE's, in addition to the initial values of the variables in the direct kinematics problem, we have to obtain the initial values of $\theta_1, \theta_2, \phi_3, \alpha, \beta, z_c$. We can choose $\theta_1 = 0, \theta_2 = 0, \phi_3 = 0$ (or any other initial desired heading). As we know $u_i, v_i, u_{g_i}, v_{g_i}, \psi_i, i = 1, 2, 3$, we can obtain the position vector of the center of the 3 wheels $\vec{OC}_1, \vec{OC}_2, \vec{OC}_3$. From three points, we can obtain the rotation matrix ${}^0_p[R]$ of the platform. Once the rotation matrix is known, the 3–2–1 Euler angle sequence, γ, β, α can be found. The position of the center of the platform is given by Eq. (8) and we have x_c, y_c and z_c at the initial instant.

4. Numerical simulation and results

We have tested our algorithm on various synthetically generated surfaces and for various types of inputs. We present one representative result (several more simulation results are available in [13]). The uneven ground (surface) used in the simulations is shown in Fig. 3 and the geometrical parameters of the WMR are as chosen follows:

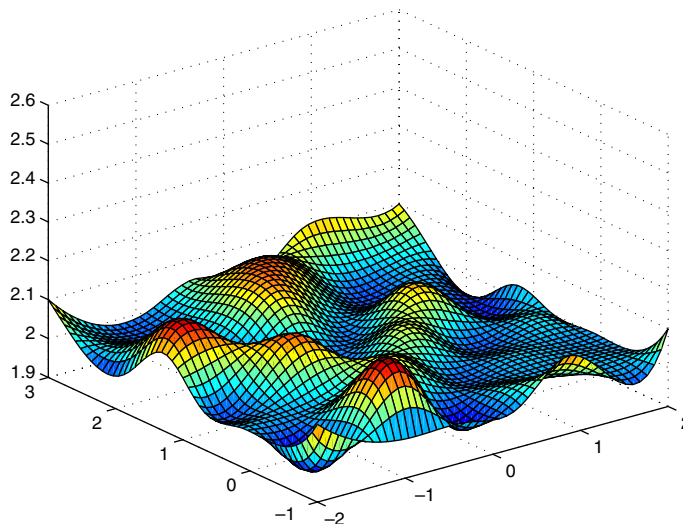


Fig. 3. Uneven terrain used for simulation.

Length of the rear axle = $2l_a = 2$ m.

Distance of center of front wheel from middle of axle = $l_s = 1.5$ m.

Two radii of the torus shaped wheel are $r_1 = 0.05$ m, $r_2 = 0.25$ m.

The center of the vehicle is assumed to be at $(1/3)l_s$ from the center of the axle along the line joining the center of the axle to the center of front wheel.

The absolute tolerance used for the solution in Matlab is 10^{-8} and the relative tolerance used is 10^{-6} .

The initial conditions for direct kinematics are computed as $\delta_1 = \delta_2 = 0$ rad, $\theta_3 = 0$ rad, $u_1 = 1.586967$ m, $v_1 = 3\pi/2$ rad, $u_{g_1} = 0.983772$ m, $v_{g_1} = -0.037978$ m, $\psi_1 = -3.140963$ rad, $u_2 = 1.547598$ rad, $v_2 = 3\pi/2$ rad, $u_{g_2} = -l_a$, $v_{g_2} = 0$ m, $\psi_2 = -3.144127$ rad, $u_3 = 1.578296$ rad, $v_3 = 3\pi/2$ rad, $u_{g_3} = 0.001578$ m, $v_{g_3} = 1.549151$ m, and $\psi_3 = -3.143452$ rad. For inverse kinematics, in addition, we have $\theta_1 = \theta_2 = \phi_3 = \alpha = 0$ rad, $\beta = 0.009$ rad, and $z_c = 2.3131$ m.

For the direct kinematics problem the inputs are chosen as $\dot{\theta}_1 = 0.5$ rad/s, $\dot{\theta}_2 = 0.4$ rad/s, $\dot{\phi}_3 = 0$ rad/s. The inputs represent constant velocity in rear wheels and constant heading (steering) angle in the front wheel. The variation of lateral tilts of the rear wheels when the 3-wheeled WMR is moving on the uneven terrain is shown in Fig. 4. The satisfaction of holonomic constraints (see Eq. 7) during motion on uneven terrain is depicted in Fig. 5, and the locus of the wheel center's, wheel-ground contact points and the center of the platform is shown in Fig. 6.

For the inverse kinematics problem, the inputs chosen are $\dot{x}_c = 0.01255$ m/s, $\dot{y}_c = 0.12865$ m/s, $\dot{\gamma} = 0.0159$ rad/s. Figs. 7–9 show variation of lateral tilt, constraint satisfaction and locus of the wheel-ground contact points and the center of the platform respectively, when the 3-wheeled WMR moves on the same uneven terrain shown in Fig. 3. It may be noted that due to the lateral

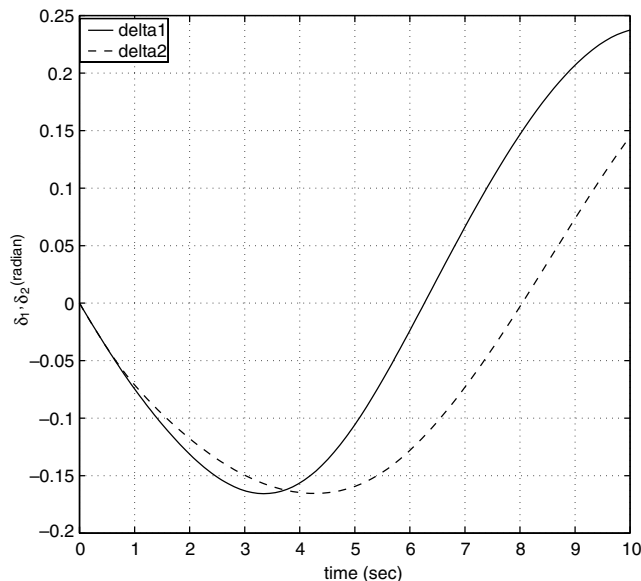


Fig. 4. Variation of lateral tilt for 3-wheeled WMR.

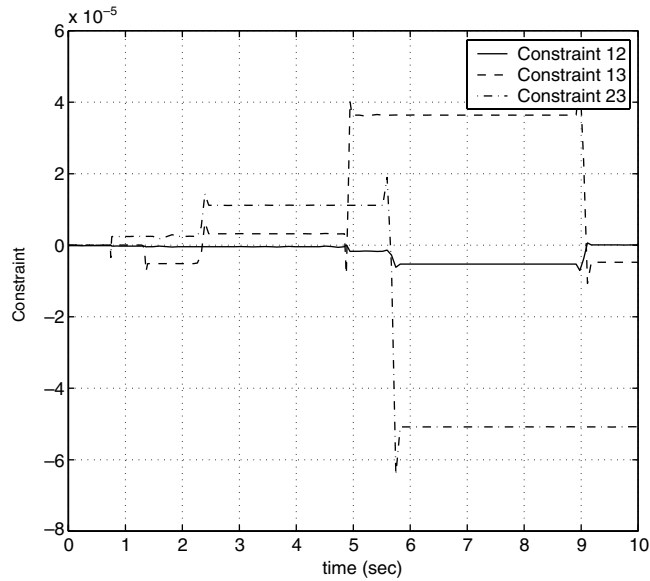


Fig. 5. Constraint satisfaction for 3-wheeled WMR.

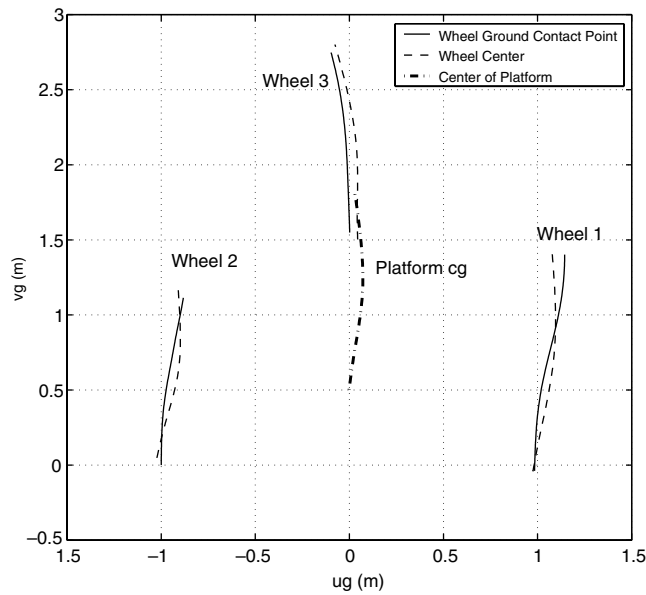


Fig. 6. Plot of wheel centers, wheel-ground contact point and platform CG.

tilt and the uneven terrain the locus of the wheel ground contact point and the centre of the wheel is different. For conventional WMR's, moving on flat terrain, the locus of the wheel-ground contact point and the wheel centre are same.

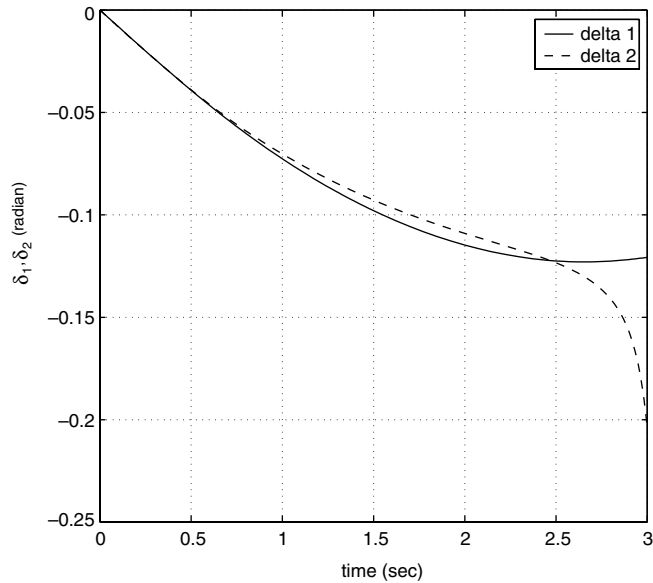


Fig. 7. Variation of lateral tilt—inverse kinematics.

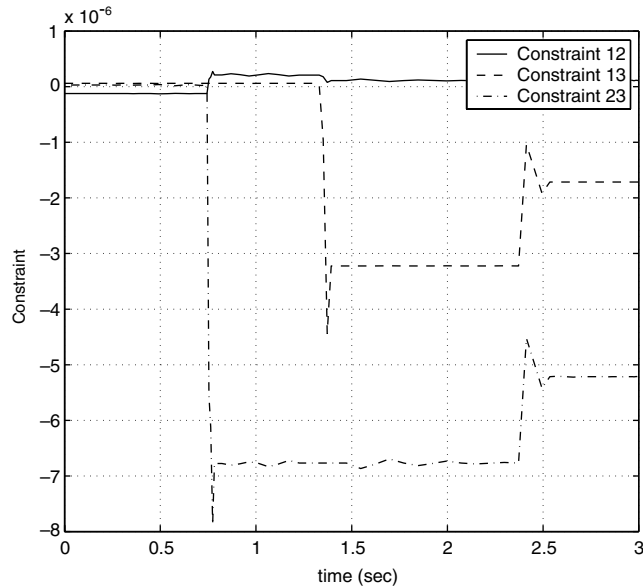


Fig. 8. Constraint satisfaction—inverse kinematics.

During the motion of the three-wheeled WMR, the slip velocities v_x and v_y are computed for each wheel. Fig. 10 shows that the no-slip conditions at the wheel ground contacts are satisfied for the direct kinematics simulation. Likewise Fig. 11 show that the no-slip condition between the wheels and the uneven ground is also satisfied for the inverse kinematics simulation.

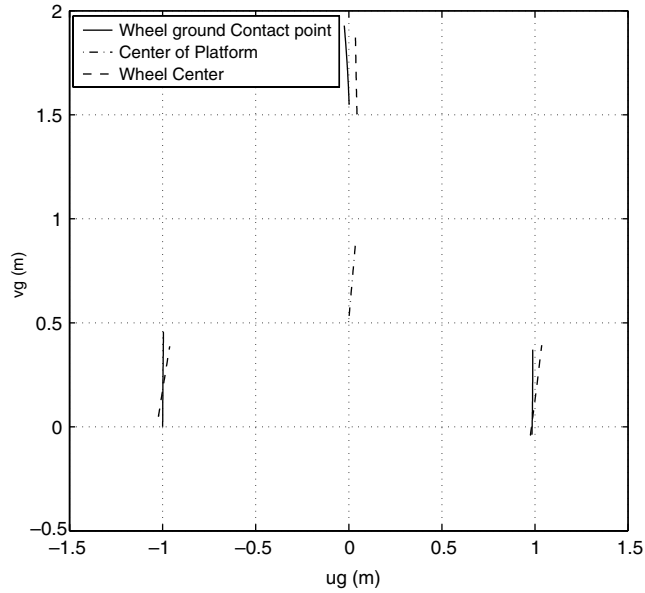


Fig. 9. Plot of wheel centers, wheel-ground contact point and platform CG—inverse kinematics.

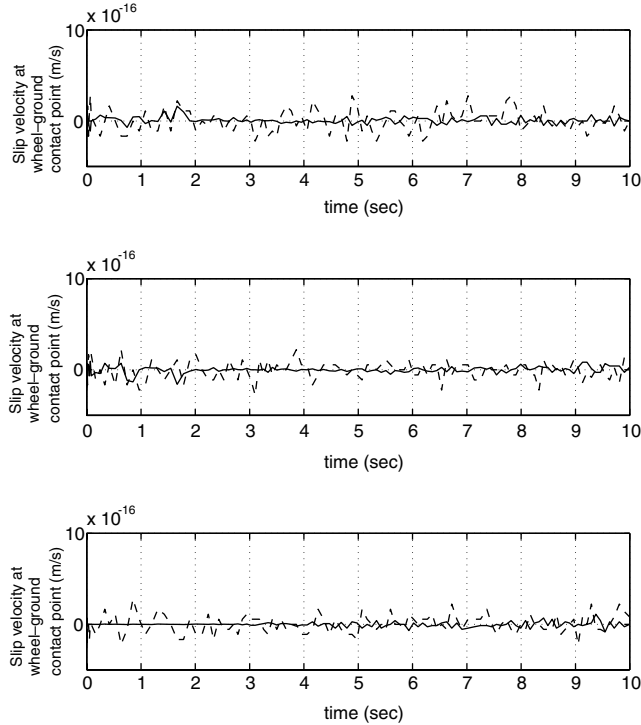


Fig. 10. Plot of v_x and v_y for each wheel—direct kinematics.

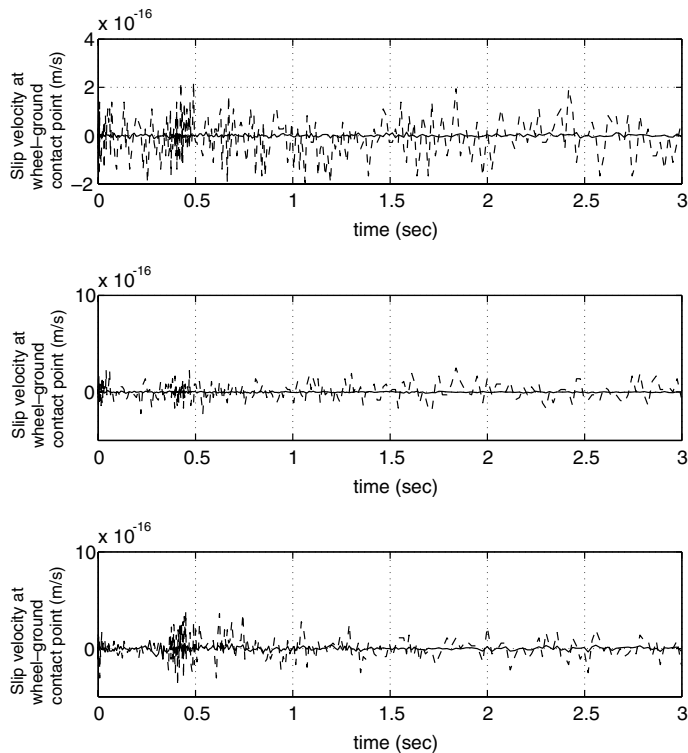


Fig. 11. Plot of v_x and v_y for each wheel—inverse kinematics.

5. Conclusion

In this paper we have studied the problem of kinematic slip for mobile robots moving on uneven terrain. We have departed from the conventional thin disk model and considered a torus shaped wheel for motion with single point contact. This enables us to take into account the lateral variation of the contact point on the wheel when moving on uneven terrain. For eliminating kinematic slip we have proposed the use of a passive joint which allows lateral tilt of the wheels. We have demonstrated our approach using a three wheeled vehicle, modeling the wheel–ground contact points as a 3-DOF joint with constraints described by ordinary differential equations. The direct and inverse kinematics problems for a three-wheeled WMR are stated and algorithms to solve the problems are presented. Numerical simulation results clearly show that the WMR modeled with torus shaped wheels and non-holonomic constraints at the wheel–ground contact, can negotiate uneven terrain without kinematic slip.

References

- [1] J.C. Alexander, J.H. Maddocks, On the kinematics of wheeled mobile robots, *Int. J. Rob. Res.* 8 (5) (1989) 15–27.
- [2] P.F. Muir, C.P. Neuman, Kinematic modeling of wheeled mobile robots, *J. Rob. Syst.* 4 (2) (1987) 281–329.
- [3] K.J. Waldron, Terrain adaptive vehicles, *Trans. ASME J. Mech. Des.* 117B (1995) 107–112.

- [4] B.J. Choi, S.V. Sreenivasan, P.W. Davis, Two wheels connected by an unactuated variable length axle on uneven ground: kinematic modeling and experiments, *Trans. ASME J. Mech. Des.* 121 (1999) 235–240.
- [5] B.J. Choi, S.V. Sreenivasan, Gross motion characteristics of articulated robots with pure rolling capability on smooth uneven surfaces, *IEEE Trans. Rob. Autom.* 15 (2) (1999) 340–343.
- [6] P.W. Davis, S.V. Sreenivasan, B.J. Choi, Kinematics of two wheels joined by a variable-length axle on uneven terrain, in: *Proc. of ASME DETC'97*, Paper no. DETC97/DAC-3857, 1997.
- [7] S.V. Sreenivasan, P. Nanua, Kinematic geometry of wheeled vehicle systems, 24th ASME Mechanisms Conference, Irvine, CA, 96-DETC-MECH-1137, 1996.
- [8] S.V. Sreenivasan, K.J. Waldron, Displacement analysis of an actively articulated wheeled vehicle configuration with extension to motion planning on uneven terrain, *Trans. ASME J. Mech. Des.* 118 (1996) 312–317.
- [9] D.J. Montana, The kinematics of contact and grasp, *Int. J. Rob. Res.* 7 (3) (1988) 17–32.
- [10] M.E. Mortenson, *Geometric Modeling*, John Wiley & Sons, 1985.
- [11] *MATLAB Users Manual*, Mathwork Inc, USA, 1992.
- [12] S. Wolfram, *The Mathematica Book*, fourth ed., Cambridge University Press, 1999.
- [13] N. Chakraborty, *Modeling of wheeled mobile robots on uneven terrain*, M.S. Thesis, Department of Mechanical Engineering, IISc Bangalore, 2003.